

A New Single-phase Static PFC Inverter Using Pre-calculated Switching Angles

K. MEGHRICHE¹, O. MANSOURI², A. CHERIFI³
 University of Versailles Saint-Quentin en Yvelines (UVSQ)
 Versailles Laboratory of Robotics (LRV),
 Integrated Systems Research Group (GRIS)
 IUT Mantes-en-Yvelines
 7, rue Jean Hoët
 78200, Mantes-La-Jolie, France.

¹meghrich@lr.v.uvsq.fr ²mansouri@lr.v.uvsq.fr ³acherifi@iut-mantes.uvsq.fr

Abstract – This paper presents a new method for static power factor correction (SPFC). A static system is used to compensate four-quadrant reactive power using only small component (capacitance) values. As such, SPFC is able to deal with inductive and/or capacitive load characteristics.

The proposed SPFC method combines a passive filter and an inverter with pre-calculated pulse-width modulation (PWM) switching angles. The obtained system produces low harmonic distortion thus providing reliable and long lasting system components.

Simulation results show that the system is able to provide variable positive and negative true and reactive powers while keeping the passive system components values constant.

Key-Words: power factor correction, single-phase inverter, static compensator, harmonic distortion, switching angles

1 Introduction

Power factor correction (PFC) has been the focus of attention for many years. Several methods have been developed based on well known circuits (Buck-boost, half-bridge, full-bridge), in an attempt to solve inherent PFC problems as caused by harmonic currents and voltages.

Harmonic distortion impairs actuators and switches as it increases eddy currents, hysteresis losses, and reduces the life time of the machine winding insulators [1, 2]. Pre-calculated pulse width modulation method is used to determine the switching angles to minimize the harmonic distortion [3].

The proposed solutions as in [4, 5, 6, 7], to name but a few, can be divided into two broad classes: dynamic PFC correction scheme through the use of a synchronous wind rotor machine (synchronous condenser), and static PFC compensation scheme consisting of switched banks of very bulky capacitors. Alternative solutions have been proposed as in [8, 9, 10] to enhance performance and/or reduce capacitors size.

It is true that the above methods have brought substantial improvement of the PFC, nevertheless, their main problem is that PFC compensation can only be performed for either inductive or capacitive load while they fail to compensate PFC for the already existing network reactive power. In this paper, we propose a novel static PFC approach that is capable of operating in the four-quadrant true-

power (hereafter denoted P) –reactive power (hereafter denoted Q) ‘PQ’ plane as shown in Fig. 1. Consequently, SPFC compensates power factor for any type of reactive power.

The remaining of the paper is organized as follows: system modeling and analysis are presented in section II; section III describes the new SPFC method using pre-calculated switching angles. Simulation results are presented in section IV. At last, a conclusion is given in section V.

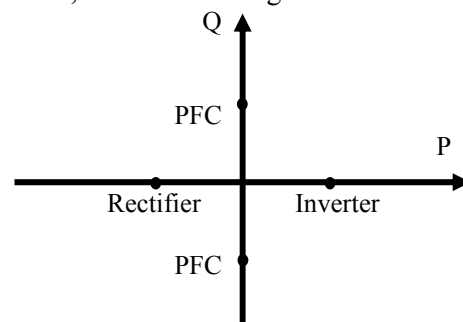


Fig. 1 Four-quadrant PQ plane

2 System Modeling and Analysis

Figure 2 shows the basic structure of a single-phase PFC inverter having E as dc voltage, \bar{V} as ac output voltage. An LC circuit is used to filter the inverter output. The inverter filtered output voltage is taken across the capacitor C (between points a and b). R represents the inductor internal resistance. T_i and T'_i ($i=1, 2$) are the semiconductor switches.

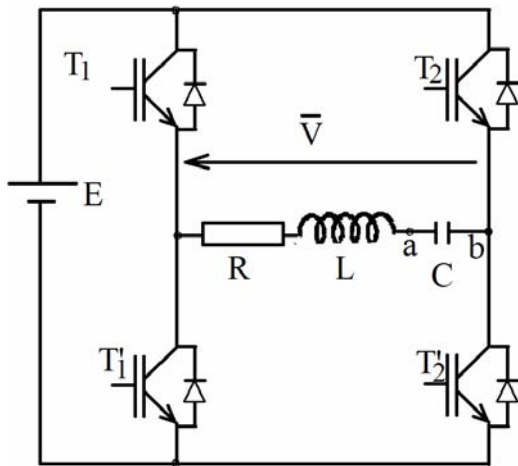


Fig. 2 Single-phase full-bridge inverter

It can be shown that the circuit of Fig. 2 can be transformed to an equivalent circuit represented in Fig. 3 as seen by the load, where \bar{E}_{Th} is the Thevenin's equivalent generator voltage.

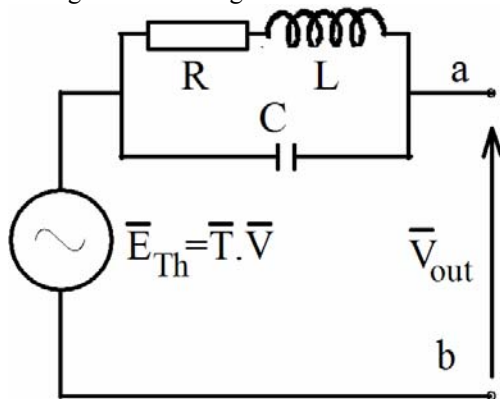


Fig. 3 Load-side equivalent circuit

From Fig. 3, one can obtain \bar{E}_{Th} as given by eq. (1).

$$\bar{E}_{Th} = \frac{\bar{V}}{1 - LC\omega^2 + jRC\omega} \quad (1)$$

This leads to the transfer function \bar{T} given by (2).

$$\bar{T} = \frac{\bar{E}_{Th}}{\bar{V}} = \frac{1}{1 - LC\omega^2 + jRC\omega} \quad (2)$$

It can be shown that the maximum of T (T_{max}), is given by (3)

$$T_{max} = \frac{1}{\sqrt{\left[1 - LC\left(\frac{1}{LC} - \frac{R^2}{2L^2}\right)^2\right] + R^2C^2\left(\frac{1}{LC} - \frac{R^2}{2L^2}\right)^2}} \quad (3)$$

that can be reduced to

$$T_{max} = \frac{L}{R^2C} \sqrt{\frac{L}{R^2C} - \frac{1}{4}} \quad (4)$$

From (4), it can be easily shown that T_{max} is always greater than 1. Consequently, the harmonic filter

behaves as an amplifying circuit for the fundamental as well. In the next section we describe the novel PFC scheme using pre-calculated switching angles.

3 New Static PFC Compensation Using Pre-calculated Switching Angles

3.1 Pre-calculated Switching Angles

In order to achieve single-phase reactive power compensation, a pre-calculated switching angles determination method similar to that developed in [3] has been used.

The objective is to determine directly the switching angles so as to obtain the best possible match between the inverter output voltage V and the desired ac voltage V_d .

For this purpose, we propose to compare their respective harmonics. A perfect matching between V and V_d is achieved only when an infinite number of harmonics is considered. Practically, the number of harmonics N that can be identical is finite. This number, to be maximized, depends on the number of switching times per period.

Figure 4 gives the algorithm used to determine the switching angles α_i from the nonlinear set of equations $a_k = d_k$, where NP is the number of parameters (switching angles).

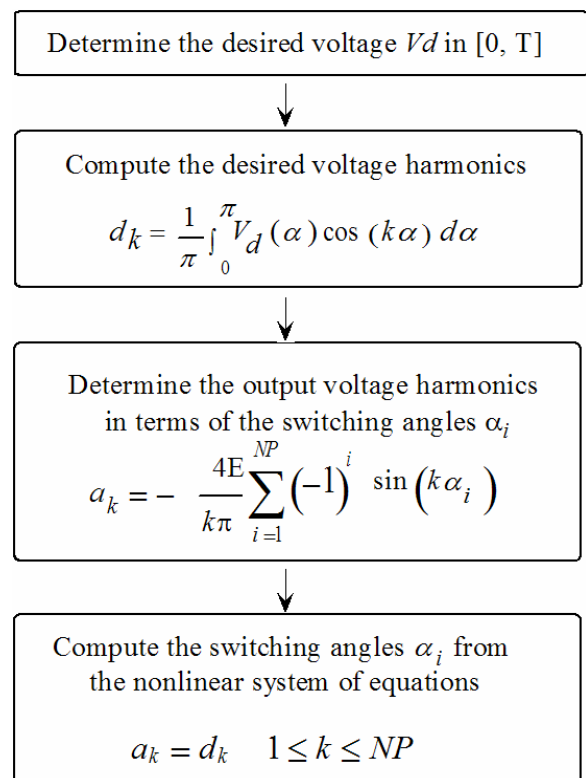


Fig. 4 Single-phase switching angles determination algorithm

3.2 Proposed SPFC

Figure 5 shows the load voltage polarity and current flow direction. One can notice that voltage and current are chosen to be of opposite direction.

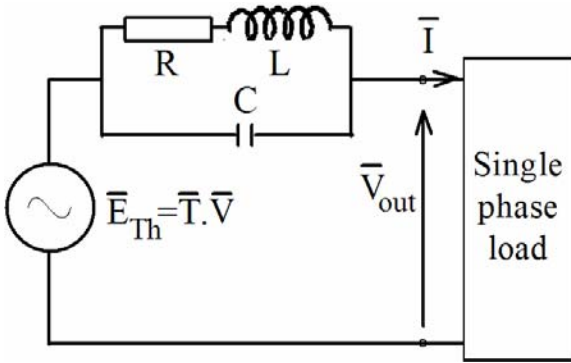


Fig. 5 Load voltage polarity and current flow direction

Depending on the sign of the instantaneous power $p = v_{out} \cdot i$, two cases may arise

- Case 1: p is positive; the power is absorbed by the load, as shown in Fig. 6(a).
- Case 2: p is negative; the power is delivered by the load as shown in Fig. 6(b).

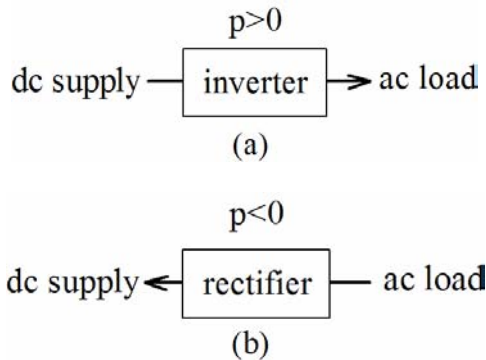


Fig. 6 Load behavior depending on the instantaneous power sign

The active and reactive load powers are given by (5).

$$\begin{cases} P = V_{out} I \cos(\varphi) \\ Q = V_{out} I \sin(\varphi) \end{cases} \quad (5)$$

where φ is the phase shift angle between the load current and voltage, $\varphi = (\bar{I}, \bar{V}_{out})$.

From Fig. 5, the generator voltage E_{Th} can be expressed as

$$\bar{E}_{Th} = \bar{V}_{out} + \frac{\bar{I}}{jC\omega + \frac{1}{R + jL\omega}} \quad (6)$$

$$\bar{E}_{Th} = \bar{V}_{out} + \frac{R + jL\omega}{1 - LC\omega^2 + jRC\omega} \bar{I} \quad (7)$$

$$\bar{E}_{Th} = \bar{V}_{out} + X I \exp(j\beta) \quad (8)$$

where

$$X = \frac{\sqrt{R^2 + (L\omega)^2}}{\sqrt{(1 - LC\omega^2)^2 + (RC\omega)^2}}$$

and

$$\begin{cases} \beta = \varphi + \alpha \\ \alpha = \alpha_1 - \alpha_2 \\ \alpha_1 = \arctg \frac{L\omega}{R} \\ \alpha_2 = \arctg \frac{RC\omega}{1 - LC\omega^2} \end{cases}$$

This is represented under phasor diagram form in Fig. 7 with δ being the phase shift angle between \bar{V}_{out} and \bar{E}_{Th} .

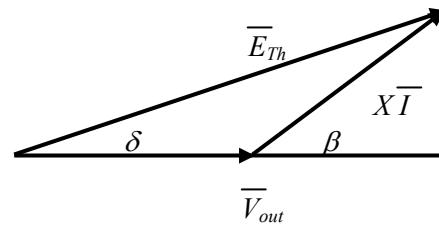


Fig. 7 \bar{E}_{Th} phasor diagram

Ultimately, (5) can be rewritten as

$$\begin{cases} P = V_{out} \left[\frac{E_{Th} \cos(\delta) - V_{out} \cos(\alpha)}{X} + \frac{E_{Th} \sin(\delta)}{X} \sin(\alpha) \right] \\ Q = V_{out} \left[\frac{E_{Th} \sin(\delta)}{X} \cos(\alpha) - \frac{E_{Th} \cos(\delta) - V_{out} \sin(\alpha)}{X} \right] \end{cases} \quad (9)$$

It is worth to remind that our main objective is to perform power factor correction meaning that the delivered power to the load must be zero.

$$P_{delivered} = 0, \text{ and } Q_{delivered} + Q_{load} = 0.$$

Consequently, (9) yields

$$\begin{cases} E_{Th} = V_{out} \frac{\cos(\alpha)}{\cos(\delta - \alpha)} \\ Q = V_{out}^2 \frac{\sin(\alpha_1) RC}{\sin(\alpha_2) L} \left[\frac{\cos(\alpha)}{\cos(\delta - \alpha)} \sin(\delta - \alpha) + \sin(\alpha) \right] \end{cases} \quad (10)$$

$$\begin{cases} E_{Th\ ref} = \frac{V_{out}}{\cos(\delta)} \\ Q = V_{out}^2 \frac{RC}{L} \tan(\delta_{ref}) = -V_{out} I_l \sin(\varphi_l) \end{cases} \quad (11)$$

where $\varphi_l = (\bar{I}_l, \bar{V}_{out})$ and I_l being the load current as illustrated in Fig. 8.

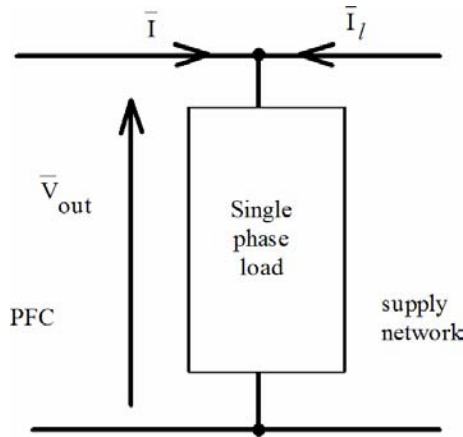


Fig. 8 PFC and supply network currents

Equation 11 shows that the delivered reactive power (Q) depends on both the capacitor C and the phase shift angle $\delta_{ref} = (\bar{V}_{out}, \bar{E}_{Th})$. By varying the δ_{ref} from $-\frac{\pi}{2}$ to $\frac{\pi}{2}$, the reactive power can be varied in the interval $]-\infty, \infty[$. This allows our SPFC scheme to compensate large reactive power using only small capacitance values. However, in the neighborhood of $\pm \frac{\pi}{2}$, the amplitude of the generator voltage will increase.

Rearranging (11), we obtain the following expressions for the reference generator voltage and phase shift angle $\delta_{ref} = (\bar{V}_{out}, \bar{E}_{Th})$.

$$\begin{cases} E_{Th\ ref} = V_{out} \sqrt{1 + \left(\frac{I_l \sin(\varphi_l)}{V_{out} \frac{RC}{L}} \right)^2} \\ \delta_{ref} = -Arctg \left[\frac{I_l \sin(\varphi_l)}{V_{out} \frac{RC}{L}} \right] \end{cases} \quad (12)$$

4 Simulation Results

Simulation is carried out using the parameters given in Table 1.

Table 1 Simulation parameters

<i>R</i>	<i>L</i>	<i>C</i>	<i>V_{out}</i>
0.1 Ω	1 mH	100 μF	230 V

where R represents the internal inductor resistance.

The load current variation is normalized from 0 to 1 and the phase angle φ_l is varied in the interval $]-\frac{\pi}{2}, \frac{\pi}{2}[$.

Taking $E_{Th} = 1000 V_{out}$ and $\delta = 1.56$ radians, the obtained results show that, SPFC is able to compensate a reactive power of 529 KVAR. For the sake of comparison, a conventional PFC scheme will be able to compensate only 1.6 KVAR as illustrated in Table 2.

Table 2: Comparative table between conventional and proposed static PFC methods

<i>Parameters</i>	<i>Compensated reactive power</i>	
$E_{Th} = 1000 V_{out}$	Conventional PFC	Proposed SPFC
Phase angle $\delta = 1.56$ rads	1.6 KVAR	529 KVAR

Figure 9 shows the reference voltage E_{Th} variation with respect to load current I_l and load phase angle φ_l . One can notice that E_{Th} increases when φ_l approaches $\pm \frac{\pi}{2}$. This increase is the cost to keep the value of capacitor C constant.

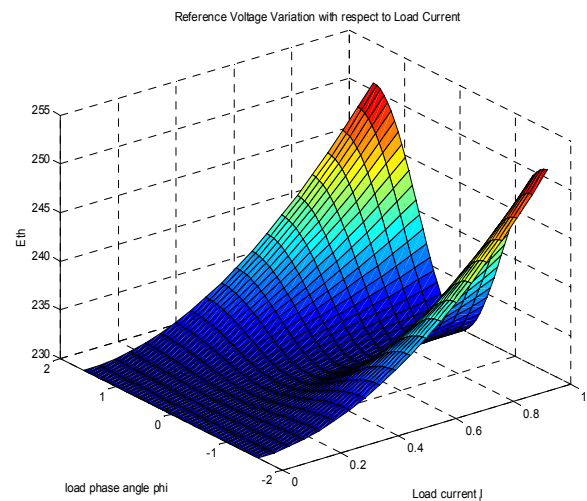


Fig. 9 Reference voltage-load current variation

Figure 10 shows the phase shift angle $\delta_{ref} = (\bar{V}_{out}, \bar{E}_{Th})$ with respect to load phase angle

φ_l and load current (I_l) variation. δ_{ref} is proportional to φ_l and I_l .

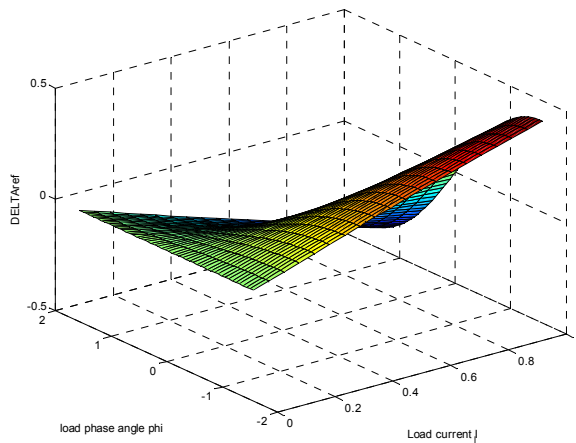


Fig. 10 δ_{ref} with respect to load current variation

Figures 11 and 12 show other 3-D views of the variations of the reference voltage E_{Th} and phase shift angle δ_{ref} respectively using another set of simulation parameters given in Table 3.

Table 3 Other simulation parameters

R	L	C	V_{out}
0.1Ω	$100 \mu\text{H}$	$200 \mu\text{F}$	230 V

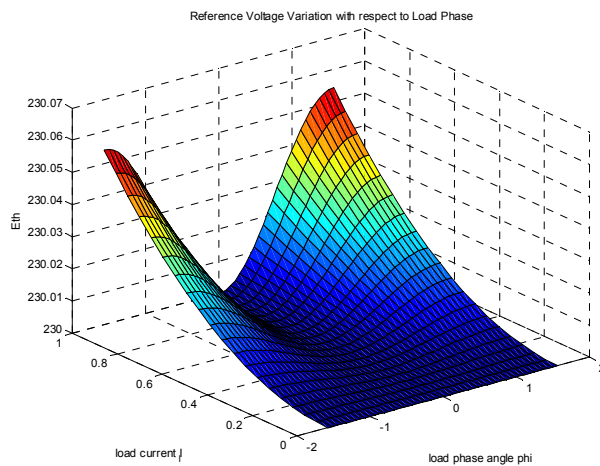


Fig. 11 Reference voltage–load phase variation

5 Conclusion

A new static PFC method based on the pre-calculated switching angles approach has been presented. The switching angles are pre-calculated by resolving a nonlinear system of equations. Compared with other methods, the proposed SPFC method is able to balance four-quadrant reactive power (load independent) using small component (mainly capacitance) values, and provides more reliable and long lasting system components due to

low harmonic distortion. It can represent a cost effective method for implementing four-quadrant PFC compensation for power systems.

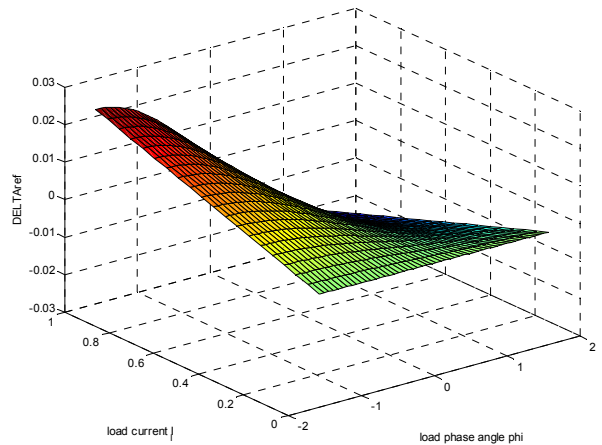


Fig. 12 δ_{ref} with respect to load phase variation

References:

- [1] F. Amrane, A. Cherifi, C. Dubuc, "A calculated PWM switching methods for three-phase inverter", in *Proc. IEEE 2000 Large Engineering Systems Conference on Power Engineering*, Halifax, July 2000, pp. 103–107
- [2] J. Holtz, M. Stamm, J. Thur and A. Linder, "High-Power Pulsewidth Controlled Current Source GTO Inverter for High Switching Frequency", in *Proc. of the 1997 IEEE Industry Applications Society Annual Meeting*, New Orleans/Miss., Oct. 1997
- [3] K. Meghriche, F. Fouzi, A. Cherifi, "A new switching angle determination method for three-leg inverter", in *Proc. IEEE Mechatronics and Robotics Conference Mechrob'04*, 13–15 Sept. 2004, Aachen, Germany, pp. 378–382
- [4] K. Matsui & al., "A comparison of various buck-boost converters and their application to PFC", in *Proc. IECON 02 Transactions on Industrial Electronics*, Vol. 1, 5–8 Nov. 2002, pp. 30–36.
- [5] Y. Nishida, S. Motegi, A. Maeda, "Single-phase buck-boost AC-to-DC converter with high-quality input and output waveforms", in *Proc. of the IEEE International Symposium on Industrial Electronics*, 1995. ISIE '95, Vol. 1, 10–14 July 1995, pp. 433–438
- [6] Gui-Jia, Donald J. Adams, Leon M. Tolbert, "Comparative study of power factor correction converters for single phase half-bridge inverters", in *Proc. IEEE 32nd Annual Power Electronics Specialists Conference PESC' 2001*, Vol. 2, 17–21 June 2001, pp. 995–1000

- [7] Sangsun Kim, Prasad N. Enjeti, "A modular single-phase power-factor-correction scheme with a harmonic filtering function", IEEE Transactions on Industrial Electronics, Vol. 50, No. 2, April 2003, pp. 328–335
- [8] V. Anunciada, B. Borges, "Power factor correction in single phase AC-DC conversion: control circuits for performance optimization", in Proc. of IEEE 35th Annual Power Electronics Specialists Conference PESC04, Vol. 5, 20–25 June 2004, pp. 3775–3779
- [9] Werner H. Wölfle, William G. Hurley, "Quasi-active power factor correction with a variable inductive filter: theory, design and practice", IEEE Trans. on Power Electronics, Vol. 18, No. 1, January 2003, pp. 248–255.
- [10] A. Lazaro, A. Barrado, J. Pleite, E. Olias, "New power factor correction AC/DC converter with reduced storage capacitor voltage", in Proc. of the IEEE Industrial Electronics Society, 28th Annual Conference of the IECON 02, Vol. 1, 5–8 Nov. 2002, pp. 353– 358